

# The Isotridecanyl Side Chain of Plusbacin-A<sub>3</sub> Is Essential for the Transglycosylase Inhibition of Peptidoglycan Biosynthesis

Sung Joon Kim,<sup>†</sup> Manmilan Singh,<sup>‡</sup> Aaron Wohlrab,<sup>§</sup> Tsyr-Yan Yu,<sup>‡</sup> Gary J. Patti,<sup>‡</sup> Robert D. O'Connor,<sup>‡</sup> Michael VanNieuwenhze,<sup>\*,§</sup> and Jacob Schaefer<sup>\*,‡</sup>

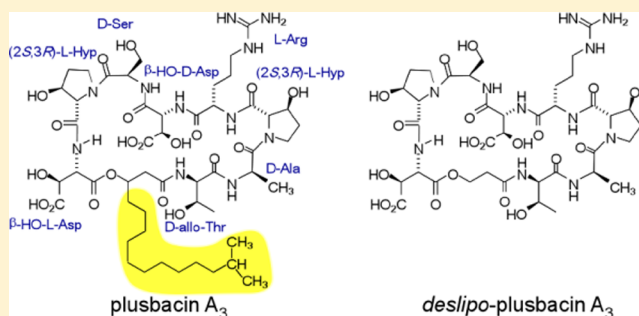
<sup>†</sup>Department of Chemistry and Biochemistry, Baylor University, Waco, Texas 76798, United States

<sup>‡</sup>Department of Chemistry, Washington University, St. Louis, Missouri 63130, United States

<sup>§</sup>Department of Chemistry, Indiana University, Bloomington, Indiana 47405, United States

## S Supporting Information

**ABSTRACT:** Plusbacin-A<sub>3</sub> (pb-A<sub>3</sub>) is a cyclic lipopeptide that exhibits antibacterial activity against multidrug-resistant Gram-positive pathogens. Plusbacin-A<sub>3</sub> is thought not to enter the cell cytoplasm, and its lipophilic isotridecanyl side chain is presumed to insert into the membrane bilayer, thereby facilitating either lipid II binding or some form of membrane disruption. Analogues of pb-A<sub>3</sub>, [<sup>2</sup>H]pb-A<sub>3</sub> and *deslipo*-pb-A<sub>3</sub>, were synthesized to test membrane insertion as a key to the mode of action. [<sup>2</sup>H]pb-A<sub>3</sub> has an isotopically <sup>2</sup>H-labeled isopropyl subunit of the lipid side chain, and *deslipo*-pb-A<sub>3</sub> is missing the isotridecanyl side chain. Both analogues have the pb-A<sub>3</sub> core structure. The loss of antimicrobial activity in *deslipo*-pb-A<sub>3</sub> showed that the isotridecanyl side chain is crucial for the mode of action of the drug. However, rotational-echo double-resonance nuclear magnetic resonance characterization of [<sup>2</sup>H]pb-A<sub>3</sub> bound to [1-<sup>13</sup>C]glycine-labeled whole cells of *Staphylococcus aureus* showed that the isotridecanyl side chain does not insert into the lipid membrane but instead is found in the staphylococcal cell wall, positioned near the pentaglycyl cross-bridge of the cell-wall peptidoglycan. Addition of [<sup>2</sup>H]pb-A<sub>3</sub> during the growth of *S. aureus* resulted in the accumulation of Park's nucleotide, consistent with the inhibition of the transglycosylation step of peptidoglycan biosynthesis.



Plusbacin-A<sub>3</sub> (pb-A<sub>3</sub>) is a cyclic lipopeptide (Figure 1, left) produced by *Pseudomonas* sp. PB-6250<sup>1</sup> that exhibits antibacterial activity with a minimal inhibitory concentration (MIC) range of 0.78–3.13  $\mu\text{g/mL}$ <sup>2</sup> against multidrug-resistant Gram-positive pathogens: vancomycin-resistant enterococci (VRE), vancomycin intermediate-resistant *Staphylococcus aureus*, and methicillin-resistant *S. aureus* (MRSA). The activity of pb-A<sub>3</sub> is antagonized by the addition of cell-wall membrane particulates, and its inhibition of nascent peptidoglycan biosynthesis in a cell membrane extract suggests that pb-A<sub>3</sub>, like vancomycin, may target the peptidoglycan precursor lipid II.<sup>2,3</sup> Unlike vancomycin, however, pb-A<sub>3</sub> is active against VRE and its activity is not affected by the addition of the tripeptide acetyl-L-Lys-D-Ala-D-Ala.<sup>2</sup> Thus, it appears that the binding site utilized by pb-A<sub>3</sub> is distinct from that of vancomycin.

The lipophilic isotridecanyl side chain of pb-A<sub>3</sub> is presumed to insert into the membrane bilayer, colocalizing the lipopeptide at the site of peptidoglycan biosynthesis and possibly facilitating some form of drug aggregation and membrane disruption.<sup>4</sup> The pb-A<sub>3</sub> analogues, *deslipo*-pb-A<sub>3</sub> and [<sup>2</sup>H]pb-A<sub>3</sub>, were synthesized to test membrane insertion as a key to the mode of action. The analogues share an identical depsipeptide core structure with pb-A<sub>3</sub>; however, *deslipo*-pb-A<sub>3</sub> (Figure 1, center) lacks the lipid side chain. [<sup>2</sup>H]pb-A<sub>3</sub> (Figure

1, right) is identical to the parent compound except for the <sup>2</sup>H labels incorporated into the isopropyl subunit of the lipid side chain. Table S1 of the Supporting Information lists the minimal inhibitory concentrations (MICs) for these analogues.

To investigate in situ pb-A<sub>3</sub> binding, we formed a complex of [<sup>2</sup>H]pb-A<sub>3</sub> with intact whole cells of *S. aureus* grown in a defined medium containing [1-<sup>13</sup>C]glycine. The localization of [<sup>2</sup>H]pb-A<sub>3</sub> in the cell wall was determined by <sup>13</sup>C{<sup>2</sup>H} rotational-echo double-resonance (REDOR) nuclear magnetic resonance (NMR).<sup>5</sup> The proposed insertion of the isotridecanyl side chain into the phospholipid membrane was investigated by <sup>31</sup>P{<sup>2</sup>H} REDOR NMR. These experiments measure the dipolar coupling between pairs of nuclei and therefore their internuclear separation.

Information about the in vivo mode of action of pb-A<sub>3</sub> was determined by adding a subinhibitory concentration of [<sup>2</sup>H]pb-A<sub>3</sub> to *S. aureus* during the midexponential growth phase in a medium containing either [1-<sup>13</sup>C]glycine and [ $\epsilon$ -<sup>15</sup>N]lysine (to label cell-wall peptidoglycan bridge links) or D-[1-<sup>13</sup>C]alanine

Received: January 7, 2013

Revised: February 18, 2013

Published: February 19, 2013



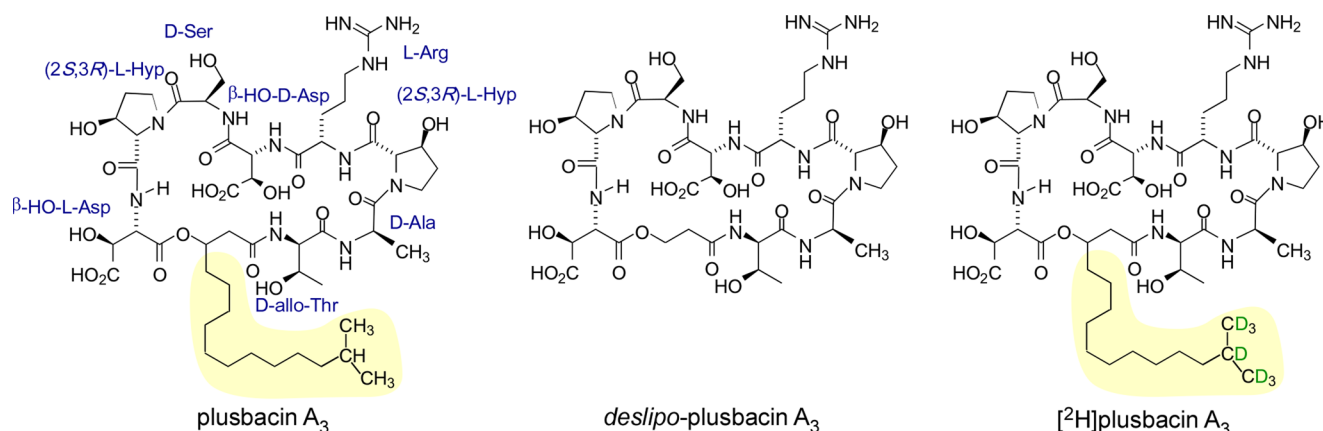


**Figure 1.** Chemical structures of pb-A<sub>3</sub>, deslipo-pb-A<sub>3</sub>, and [<sup>2</sup>H]pb-A<sub>3</sub>.

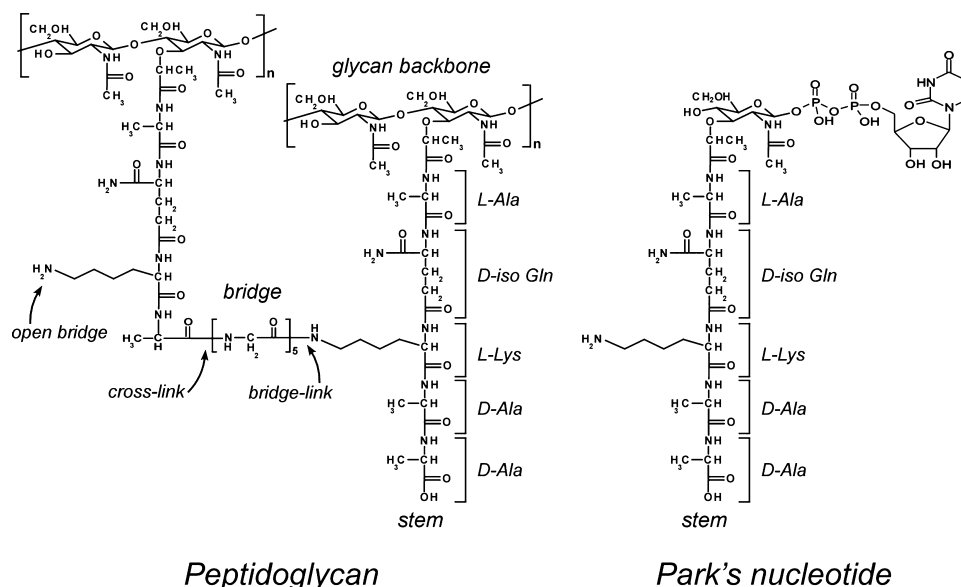


**Figure 2.** Chemical structure of *S. aureus* peptidoglycan. The repeat unit on the right is an un-cross-linked stem having the sequence L-Ala-D-iso-Gln-L-Lys-D-Ala-D-Ala. The pentaglycyl bridge attached to the  $\epsilon$ -nitrogen of L-lysine is cross-linked to the peptide stem on the left. Chemical structure of the cytoplasmic peptidoglycan precursor Park's nucleotide.

and [<sup>15</sup>N]glycine (to label cross-links) (Figure 2, left). The drug-treated *S. aureus* whole cells were harvested after being grown for 1 h, and the effects of the drug on cell-wall compositions were analyzed by <sup>13</sup>C{<sup>15</sup>N} and <sup>15</sup>N{<sup>13</sup>C} REDOR NMR.

## MATERIALS AND METHODS

**Synthesis of Plusbacin-A<sub>3</sub>.** The detailed chemical synthesis of [<sup>2</sup>H]pb-A<sub>3</sub> is presented in the Supporting Information.

**Susceptibility Testing.** Minimal inhibitory concentrations (MICs) for pb-A<sub>3</sub>, deslipo-pb-A<sub>3</sub>, and [<sup>2</sup>H]pb-A<sub>3</sub> against *Streptococcus pyogenes* M49 strain NZ131, *Streptococcus agalactiae* strain A909, MRSA (ATCC 33591), VRE (ATCC 51299), *Escherichia coli* (ATCC 25922), and *Pseudomonas aeruginosa* (ATCC 27853) were determined by the micro-dilution method recommended by the National Committee for Clinical Laboratory Standards (Table S1 of the Supporting Information).

**Growth and Labeling of Whole Cells and Formation of the Drug Complex.** A starter culture of *S. aureus* (ATCC 6538P) was grown overnight in 5 mL of trypticase soy broth at

37 °C with 250 rpm shaking and added (1% final volume) to a 1 L flask containing 335 mL of a defined medium<sup>6</sup> with the naturally abundant amino acid glycine replaced with isotope-labeled [<sup>13</sup>C]glycine to incorporate the <sup>13</sup>C-specific label at the pentaglycyl cross-bridge of the peptidoglycan (Figure 2, left). *S. aureus* was harvested under stationary-phase growth (OD<sub>660</sub> at 1.0) as described previously<sup>6</sup> and then resuspended in 7 mL of 40 mM triethanolamine buffer. In 2 mL of water was dissolved 3.9 mg of [<sup>2</sup>H]pb-A<sub>3</sub> (MW 1165.32) that had been added dropwise to the cell suspension with gentle stirring. The bacteria/pb-A<sub>3</sub> mixture was equilibrated for 6 min prior to being frozen and lyophilized.

**[<sup>2</sup>H]pb-A<sub>3</sub> Addition during Growth of *S. aureus*.** *S. aureus* was grown in four 1 L flasks each containing 330 mL of a defined medium<sup>6</sup> containing isotope-labeled [<sup>13</sup>C]glycine and L-[<sup>15</sup>N]lysine for the <sup>13</sup>C–<sup>15</sup>N pair labeling of the bridge link or D-[<sup>13</sup>C]alanine and [<sup>15</sup>N]glycine in the presence of alanine racemase inhibitor alaphosphin (5 μg/mL) for <sup>13</sup>C–<sup>15</sup>N pair labeling of the cross-link of peptidoglycan (Figure 2, left). [<sup>2</sup>H]pb-A<sub>3</sub> was added to *S. aureus* during the midexponential growth phase (OD<sub>660</sub> at 0.5) to a final concentration of 11.8

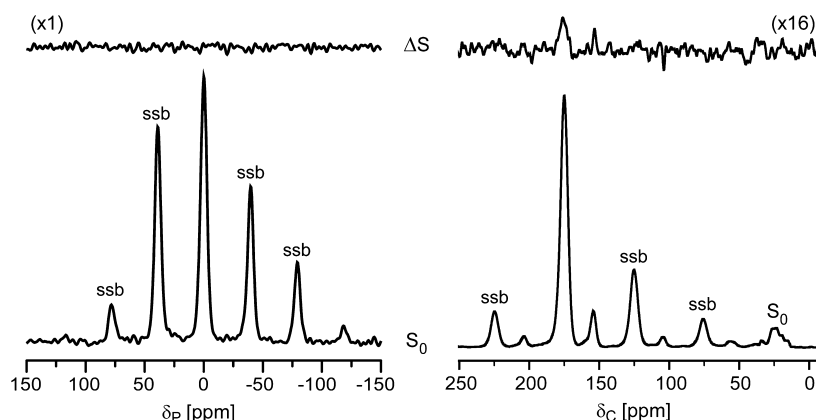


**Figure 3.** (Left) 202.4 MHz  $^{31}\text{P}\{^2\text{H}\}$  REDOR spectra of  $[^2\text{H}]\text{pb-A}_3$  complexes of whole cells of *S. aureus* after dipolar evolution of 20.0 ms. The full-echo spectrum ( $S_0$ ) is at the bottom of the figure and the REDOR difference ( $\Delta S$ ) at the top. The spectra were the result of the accumulation of 378664 scans. Magic-angle spinning was conducted at 8000 Hz. The absence of dephasing indicates that  $[^2\text{H}]\text{pb-A}_3$  did not embed in the membrane. (Right) 125 MHz  $^{13}\text{C}\{^2\text{H}\}$  REDOR spectra of  $[^2\text{H}]\text{pb-A}_3$  complexes of whole cells of *S. aureus* grown in a defined medium containing  $[1\text{-}^{13}\text{C}]\text{glycine}$  after dipolar evolution for 31.4 ms. The spectra were the result of the accumulation of 249660 scans. Magic-angle spinning was conducted at 6250 Hz. The dephasing indicates that the isotridecanoyl side chain of  $[^2\text{H}]\text{pb-A}_3$  is found near the pentaglycyl bridge segment of *S. aureus* peptidoglycan. Spinning side bands are marked as ssb.

$\mu\text{g/mL}$ . The cells were harvested by centrifugation after being grown for 1 h. The harvested cells were resuspended in 7 mL of 40 mM triethanolamine buffer and lyophilized.

**Internuclear Proximities.** REDOR was used to determine dipolar couplings and hence internuclear distances.<sup>5</sup> REDOR is a difference experiment in which two spectra are collected,  $S_0$  (full echo) and  $S$  (dephased echo). Dipolar evolution over the rotor period in the  $S$  spectrum results in reduced (dephased) peak intensity for spin pairs that are dipolar coupled. From the difference in signal intensity (REDOR difference;  $\Delta S = S_0 - S$ ) and the experimental dephasing time (the dipolar evolution time), the heteronuclear dipolar coupling and corresponding internuclear distance can be directly calculated.<sup>5</sup>

**Solid-State NMR.** The  $^{31}\text{P}\{^2\text{H}\}$  and  $^{13}\text{C}\{^2\text{H}\}$  REDOR spectra of Figure 3 were recorded using an 89 mm bore, 12 T static field ( $^1\text{H}$  at 500 MHz, Magnex, Agilent, Santa Clara, CA), with a Tecmag (Houston, TX) Apollo spectrometer, and four-channel transmission-line probes equipped with either 4 mm (Figure 3, left) or 5 mm (Figure 3, right) Chemagnetics/Varian stators and zirconium rotors. Radiofrequency pulses for  $^1\text{H}$  were amplified first by a 50 W American Microwave Technology (AMT, Anaheim, CA) power amplifier and then by a 2 kW Creative Electronics tube amplifier. One-kilowatt AMT amplifiers were used for  $^{31}\text{P}$  and  $^{13}\text{C}$  pulses. For  $^2\text{H}$ , a 2 kW AMT amplifier was used. The  $\pi$  pulse lengths were 6  $\mu\text{s}$  for  $^{31}\text{P}$ ,  $^{13}\text{C}$ , and  $^2\text{H}$ . The  $^1\text{H}$  decoupling field was 100 kHz throughout dipolar evolution and data acquisition with TPPM of the  $^1\text{H}$  radiofrequency.<sup>8</sup>

The  $^{13}\text{C}\{^{15}\text{N}\}$  and  $^{15}\text{N}\{^{13}\text{C}\}$  REDOR spectra of Figures 4–7 and Figure S3 of the Supporting Information were recorded at a spinning speed of 5 kHz in a 4.7 T, 89 mm Oxford magnet (200 MHz) (Cambridge, England), using a Tecmag Libra pulse generator and a four-channel transmission-line probe with a Chemagnetics 7.5 mm stator. One-kilowatt amplifiers were used for all frequencies. The  $\pi$  pulse lengths were 10  $\mu\text{s}$  for  $^{13}\text{C}$  and  $^{15}\text{N}$ . Cross-polarization transfers were conducted at 50 kHz for 2 ms, and  $^1\text{H}$  decoupling was at 98 kHz throughout dipolar evolution and data acquisition.

All spinning rates were actively controlled to  $\pm 2$  Hz. Similarly, all RF field amplitudes were under active control to eliminate long-term drifts due to component aging or changes

in temperature.<sup>9</sup> Additionally, alternating scans of  $S_0$  and  $S$  were acquired to compensate for short-term drift. XY-8 phase cycling<sup>10</sup> was used for all refocusing and dephasing pulses.<sup>11</sup>

**Calculations.** REDOR dephasing for spin-half pairs was calculated using the analytical expressions of Mueller et al.<sup>12</sup> REDOR dephasing for the rapidly rotating  $\text{CD}_3$  dephaser was approximated as a single super spin centered in the triangle defined by the three  $^2\text{H}$  nuclei.<sup>13–15</sup> The abbreviation  $^2\text{H}_3$  is used to denote the super spin. For both these calculations, fits of  $\Delta S/S_0$  as a function of dephasing time yield the dipolar coupling constant and hence the internuclear distance.

## RESULTS

**Antimicrobial Activities of pb-A<sub>3</sub>, deslipo-pb-A<sub>3</sub>, and  $[^2\text{H}]\text{pb-A}_3$ .** The MICs of pb-A<sub>3</sub>, deslipo-pb-A<sub>3</sub>, and  $[^2\text{H}]\text{pb-A}_3$  against Gram-positive and Gram-negative bacteria are listed in Table S1 of the Supporting Information. pb-A<sub>3</sub> exhibits a MIC range of 0.2–6.25  $\mu\text{g/mL}$  against the Gram-positive bacteria: *St. pyogenes* M49 strain NZ131, *St. agalactiae* strain A909, MRSA (ATCC 33591), and VRE (ATCC 51299). However, it is inactive against Gram-negative organisms, *E. coli* (ATCC 25922), and *P. aeruginosa* (ATCC 27853). deslipo-pb-A<sub>3</sub> has no activity in the strains examined. The  $^2\text{H}$  incorporation in  $[^2\text{H}]\text{pb-A}_3$  did not alter any pb-A<sub>3</sub> antimicrobial properties.

**$[^2\text{H}]\text{pb-A}_3$  Membrane Anchor.** The 202.4 MHz  $^{31}\text{P}\{^2\text{H}\}$  REDOR spectra of  $[^2\text{H}]\text{pb-A}_3$  complexed with  $[1\text{-}^{13}\text{C}]\text{glycine}$ -labeled whole cells of *S. aureus* after dipolar evolution for 20 ms are shown in Figure 3 (left). The  $\text{P}\{\text{D}\}$  detection range was 10 Å for these experiments. This estimate is based on a  $\Delta S/S_0$  of  $<2\%$ , or 2 times the noise level for the sum of the centerband and first two spinning side bands (Figure 3, left), where  $\sim 20\%$  of  $S_0$  is due to  $^{31}\text{P}$  in the bilayer and the remainder is mostly wall and lipoteichoic acids (see Figure 8 of ref 7). A fully extended 11-carbon side chain has a length of 8–10 Å.<sup>16</sup> Thus, the absence of dipolar contact between  $^2\text{H}_3$  and the natural abundance  $^{31}\text{P}$  of the lipid headgroups in the REDOR difference spectrum (Figure 3, top left) rules out insertion of the isotridecanoyl tail of  $[^2\text{H}]\text{pb-A}_3$  into the lipid bilayer.

**$[^2\text{H}]\text{pb-A}_3$  Binding to  $[1\text{-}^{13}\text{C}]\text{Glycine}$ -Labeled Whole Cells.** Figure 3 (right) shows 125 MHz  $^{13}\text{C}\{^2\text{H}\}$  REDOR

spectra after dipolar evolution for 31.4 ms. In the  $\Delta S$  spectrum, the glycyl carbonyl carbon positioned at 172 ppm is dephased by 1%, indicating that  $[^2\text{H}]\text{pb-A}_3$  is localized within the cell wall. The estimated asymptotical REDOR dephasing limit is a product of (i) drug binding site occupancy, (ii) the fraction of peptidoglycan stems with a glycyl bridge attached, and (iii) the fraction of glycine found in the cell wall.

To determine the first factor, the  $[^2\text{H}]\text{pb-A}_3$  binding site occupancy, we estimated the total number of peptidoglycan stems found in whole cells of *S. aureus*. On the basis of a vancomycin binding assay,<sup>7</sup> we estimated that 14.3  $\mu\text{mol}$  of peptidoglycan stems is present in whole cells of *S. aureus* grown in 335 mL of a defined medium harvested at an  $\text{OD}_{660}$  of 1.0. This is a sum of un-cross-linked peptidoglycan stems terminating in D-Ala-D-Ala (6.6  $\mu\text{mol}$ ) and cross-linked stems (7.7  $\mu\text{mol}$ ). Therefore, for 3.9 mg of  $[^2\text{H}]\text{pb-A}_3$  (3.4  $\mu\text{mol}$ ) complexed to whole cells, the estimated binding site occupancy is 24% (3.4  $\mu\text{mol}/14.3 \mu\text{mol}$ ).

The second factor, the fraction of stems with a pentaglycyl bridge attached, is approximately 85% for cells harvested under stationary-phase conditions.<sup>7</sup> The third factor, the fraction of glycine found in the cell wall of *S. aureus*, was determined from  $^{13}\text{C}\{^{15}\text{N}\}$  REDOR spectra of whole cells of *S. aureus* labeled with  $[1-^{13}\text{C}]\text{glycine}$  and  $\text{L-}[\epsilon-^{15}\text{N}]\text{lysine}$  (Figure 4, left). During a dipolar evolution of 1.6 ms, only the peptide-bonded  $^{13}\text{C}-^{15}\text{N}$  spin pairs from the peptidoglycan bridge link,  $[1-^{13}\text{C}]\text{glycine-L-}[\epsilon-^{15}\text{N}]\text{lysine}$ , appear at 172 ppm in the  $\Delta S$  spectrum. (This ignores the minor natural abundance  $^{13}\text{C}$

contribution to  $S_0$ .) The dephased 172 ppm intensity (13%) multiplied by 5 to account for the total number of glycines found in a pentaglycyl bridge means that 65% of the  $[1-^{13}\text{C}]\text{glycine}$  label in whole cells of *S. aureus* is found in the cell wall. Thus, the estimated maximal  $^{13}\text{C}\{^2\text{H}\}$  REDOR dephasing limit is  $(0.24)(0.85)(0.65) = 13\%$ . Depending on the position of the  $^2\text{H}$ , multiple glycyl carbonyl carbons in the pentaglycyl bridge can dephase. If we assume only one carbonyl carbon dephases, the dephasing limit is 2.6% (13%/5), and the corresponding  $^{13}\text{C}-^2\text{H}_3$  distance for the measured  $^{13}\text{C}\{^2\text{H}\}$  REDOR dephasing of 1% after dipolar evolution for 31.4 ms is 7 Å.

The addition of  $[^2\text{H}]\text{pb-A}_3$  did not affect the incorporation of  $[1-^{13}\text{C}]\text{glycine}$  into the cell wall as evident by the equal 172 ppm dephasing of 13% measured for both drug-treated and untreated *S. aureus* (Figure 4). Instead,  $[^2\text{H}]\text{pb-A}_3$ -treated *S. aureus* shows a smaller-amplitude purine peak at 149 ppm in the  $S_0$  spectrum (Figure 4, inset).

**Addition of  $[^2\text{H}]\text{pb-A}_3$  to Growing *S. aureus* Labeled with  $[1-^{13}\text{C}]\text{Glycine}$  and  $\text{L-}[\epsilon-^{15}\text{N}]\text{Lysine}$ .** Figure 5 shows

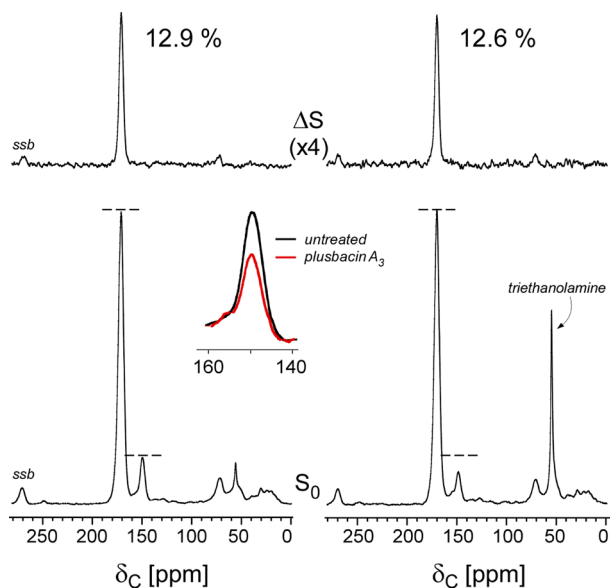


**Figure 4.** 50.3 MHz  $^{13}\text{C}\{^{15}\text{N}\}$  REDOR spectra after dipolar evolution for 1.6 ms of whole cells of *S. aureus* grown on a defined medium containing  $[1-^{13}\text{C}]\text{glycine}$  and  $\text{L-}[\epsilon-^{15}\text{N}]\text{lysine}$  in the absence (left) and presence (right) of  $[^2\text{H}]\text{pb-A}_3$  (11.8  $\mu\text{g}/\text{mL}$ ). The full-echo spectra ( $S_0$ ) are at the bottom of the figure and the REDOR differences ( $\Delta S$ ) at the top. Magic-angle spinning was conducted at 5000 Hz. Identical 172 ppm dephasing of 13% in the  $\Delta S$  spectra for *S. aureus* grown in the absence and presence of the lipopeptide indicates that  $[^2\text{H}]\text{pb-A}_3$  did not target the *fem* factors associated with pentaglycyl bridge formation. The reduced 149 ppm peak intensity in the  $S_0$  spectrum of *S. aureus* grown in the presence of  $[^2\text{H}]\text{pb-A}_3$  (highlighted in the inset) was consistent with the inhibition of  $[1-^{13}\text{C}]\text{glycine}$  metabolism in purine biosynthesis. The spectra were the result of the accumulation of 10000 scans. Spinning side bands are marked as ssb.

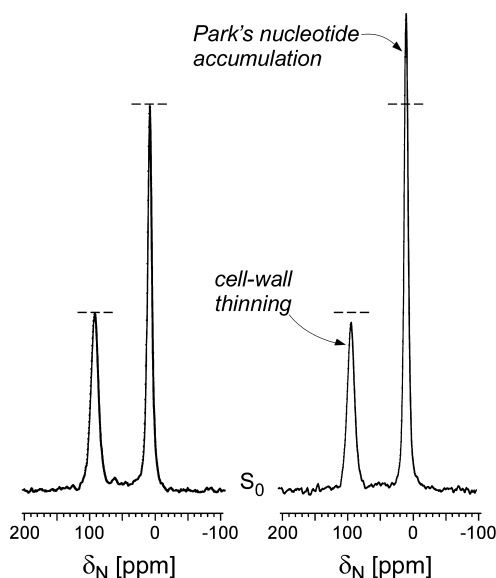


**Figure 5.** 20.3 MHz  $^{15}\text{N}\{^{13}\text{C}\}$  REDOR full-echo spectra after dipolar evolution for 1.6 ms of whole cells of *S. aureus* grown on a defined medium containing  $[1-^{13}\text{C}]\text{glycine}$  and  $\text{L-}[\epsilon-^{15}\text{N}]\text{lysine}$  in the absence (left) and presence (right) of  $[^2\text{H}]\text{pb-A}_3$  (11.8  $\mu\text{g}/\text{mL}$ ). The drug-treated *S. aureus* shows reduced lysyl-amide peak intensity at 93 ppm (cell-wall thinning) and increased lysyl-amine peak intensity at 9 ppm (accumulation of Park's nucleotide). The spectra were normalized with respect to equal sample weight and scans and were each the result of the accumulation of 20000 scans. Magic-angle spinning was conducted at 5000 Hz.

20.3 MHz  $^{15}\text{N}\{^{13}\text{C}\}$  REDOR  $S_0$  spectra of whole cells of *S. aureus* grown in a defined medium containing  $[1-^{13}\text{C}]\text{glycine}$  and  $\text{L-}[\epsilon-^{15}\text{N}]\text{lysine}$  without (left) and with (right) the addition of  $[^2\text{H}]\text{pb-A}_3$  during growth. The  $S_0$  spectra were scaled by a factor determined from  $^{13}\text{C}$  spectra shown in Figure 4 to normalize the natural abundance lipid peak intensities found at 10–30 ppm.

The addition of  $[^2\text{H}]\text{pb-A}_3$  during *S. aureus* growth diminished the 95 ppm lysyl amide peak intensity, consistent with  $[^2\text{H}]\text{pb-A}_3$  inhibition of cell-wall biosynthesis, and increased the 9 ppm lysyl amine peak intensity, which indicates



an accumulation of the cytoplasmic peptidoglycan precursor, Park's nucleotide (Figure 2, right). The inhibition of purine biosynthesis by  $[^2\text{H}]\text{pb-A}_3$  (Figure 4) is also consistent with transglycosylase inhibition in which all available glycine is routed to peptidoglycan biosynthesis, thereby indirectly preventing  $[1\text{-}^{13}\text{C}]\text{glycine}$  incorporation in the purine biosynthetic pathway.<sup>17,18</sup> These results are identical to those obtained with vancomycin, a known transglycosylase inhibitor.<sup>17,18</sup> Thus,  $\text{pb-A}_3$  also appears to be a transglycosylase inhibitor.

**Addition of  $[^2\text{H}]\text{pb-A}_3$  to Growing *S. aureus* Labeled with  $\text{D-}[1\text{-}^{13}\text{C}]\text{Alanine}$  and  $[^{15}\text{N}]\text{Glycine}$ .** The  $\text{D-}[1\text{-}^{13}\text{C}]\text{-alanine}$  incorporated into the cell wall appears at 175 ppm in the  $S_0$  spectra of the 50.3 MHz  $^{13}\text{C}\{^{15}\text{N}\}$  REDOR spectra shown in Figure 6 (bottom). The alanine racemase inhibitor,

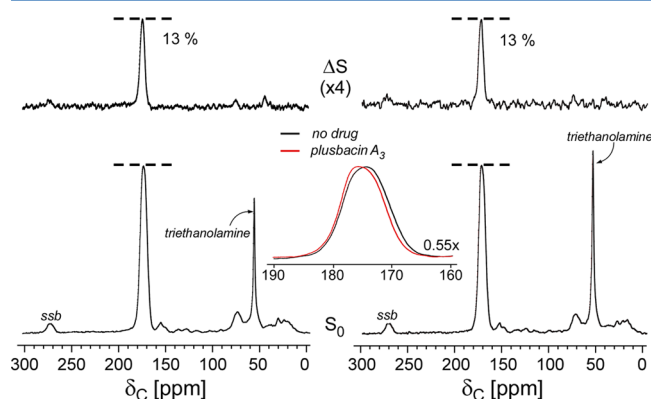


**Figure 6.** 50.3 MHz  $^{13}\text{C}\{^{15}\text{N}\}$  REDOR spectra after dipolar evolution for 1.6 ms of whole cells of *S. aureus* grown on a defined medium containing  $\text{D-}[1\text{-}^{13}\text{C}]\text{alanine}$  and  $[^{15}\text{N}]\text{glycine}$  in the absence (left) and presence (right) of  $[^2\text{H}]\text{pb-A}_3$ . The full-echo spectra ( $S_0$ ) are at the bottom of the figure and the REDOR differences ( $\Delta S$ ) at the top. The 175 ppm peak in the  $\Delta S$  spectra is from the cross-link of the peptidoglycan in the cell wall of *S. aureus*. The addition of  $[^2\text{H}]\text{pb-A}_3$  during the growth of *S. aureus* did not inhibit the transpeptidase activity of peptidoglycan biosynthesis in *S. aureus*, and therefore, the dephasing of the 175 ppm peak intensity was not affected. The inset is an expansion of the superimposed carbonyl carbon  $S_0$  spectra of *S. aureus* grown in the presence (red) and absence (black) of  $[^2\text{H}]\text{pb-A}_3$ . The addition of  $[^2\text{H}]\text{pb-A}_3$  affected the line shape of the  $^{13}\text{C}$  carbonyl spectrum centered at 175 ppm. The spectra were the result of the accumulation of 10000 scans. Spinning side bands are marked as ssb.

alaphosphin (5  $\mu\text{g}/\text{mL}$ ), prevents the racemic scrambling of  $\text{D-}[1\text{-}^{13}\text{C}]\text{alanine}$  to its enantiomeric L-form.<sup>6,7</sup> During the short dipolar evolution period of 1.6 ms, only the peptide-bonded  $^{13}\text{C}\text{--}^{15}\text{N}$  spin pairs from amino acids having the sequence  $\text{D-}[1\text{-}^{13}\text{C}]\text{Ala-}[^{15}\text{N}]\text{Gly}$  (peptidoglycan cross-link) appear in the  $\Delta S$  spectrum. The addition of  $[^2\text{H}]\text{pb-A}_3$  (11.8  $\mu\text{g}/\text{mL}$ ) did not change the  $\Delta S$  175 ppm peak intensity (Figure 6, top), and therefore, transpeptidase activity was not inhibited.

Figure S3 of the Supporting Information shows  $^{15}\text{N}\{^{13}\text{C}\}$  REDOR spectra after dipolar evolution for 1.6 ms where dephasing of the  $[^{15}\text{N}]\text{glycyl-amide}$  peak, which is also directly proportional to the extent of cross-linking in whole cells, was not affected by the addition of  $[^2\text{H}]\text{pb-A}_3$ , consistent with the  $^{13}\text{C}\{^{15}\text{N}\}$  results of Figure 6 for the same sample.

The superimposed enlarged carbonyl carbon regions of the full-echo ( $S_0$ ) spectra of *S. aureus* cells grown with (red line) and without (black line)  $[^2\text{H}]\text{pb-A}_3$  are shown in Figure 6 (inset). The differing line shapes in the 175 ppm region

indicate differences in the cell-wall composition. Figure 7 (bottom) shows the spectral subtraction of the 175 ppm full-

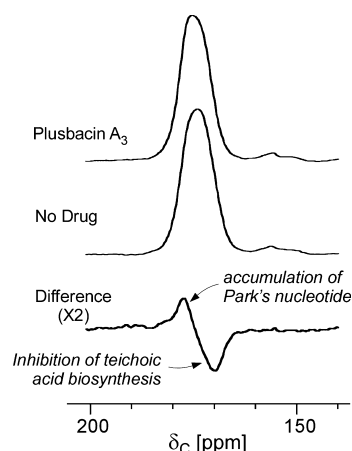


**Figure 7.** Enlargements of the carbonyl carbon region of the  $S_0$  spectra shown in Figure 6. The full-echo spectrum for *S. aureus* grown in the presence of  $[^2\text{H}]\text{pb-A}_3$  (top) is subtracted from the full-echo spectrum without the addition of drug (middle). The difference spectrum (bottom) shows a positive peak at 178 ppm due to the penultimate  $\text{D-Ala}$  carbonyl carbon of the increased level of Park's nucleotide and a negative peak at 170 ppm due to ester-linked  $\text{D-Ala}$  incorporated into teichoic acid.

echo spectrum of *S. aureus* cells grown in the presence of  $[^2\text{H}]\text{pb-A}_3$  (Figure 7, top) from the full-echo spectrum of untreated *S. aureus* cells (Figure 7, middle). The difference spectrum shows two distinct components: a positive peak at 178 ppm and a negative peak at 170 ppm. The positive 178 ppm peak is assigned to the carboxyl terminus of the penultimate  $\text{D-Ala}$ , associated with an accumulation of Park's nucleotide in the cytoplasm caused by transglycosylase inhibition.<sup>18</sup> The negative 170 ppm peak corresponds to a decreased level of ester-linked  $\text{D-}[1\text{-}^{13}\text{C}]\text{alanine}$  found in cell-wall teichoic acid.<sup>19</sup>

## DISCUSSION

The chemical structure of plusbacin consists of a cyclic depsipeptide core with a lipophilic side chain. This is a common structural motif found in numerous natural products of cyclic antimicrobial (depsi)peptides, including the calcium-dependent antibiotic complex A54145, friulimycin/amphomycin, laspartomycin, ramoplanin, fusaricidin, empedopeptin, and daptomycin.<sup>20</sup> The mode of action for most of these natural products is not well-known, but for daptomycin (Cubicin), the lipophilic side chain is thought to mediate the formation of drug oligomers that form a pore structure in the bacterial membrane.<sup>4,21</sup> The ensuing bacterial membrane depolarization is generally accepted as the killing mechanism for daptomycin, and daptomycin-related natural products. The isotridecanyl side chain of  $\text{pb-A}_3$  was presumed to play a similar role in targeting the bacterial membrane.

For  $[^2\text{H}]\text{pb-A}_3$  complexed to intact whole cells of *S. aureus*,  $\text{P}\{\text{D}\}$  REDOR showed that  $[^2\text{H}]\text{pb-A}_3$  was not embedded in the membrane (Figure 3, left). This result is consistent with the absence of lipid natural abundance  $^{13}\text{C}$  aliphatic carbon  $\text{C}\{\text{D}\}$  dephasing by  $[^2\text{H}]\text{pb-A}_3$  (Figure 3, right), which would have been expected from an embedded  $^2\text{H}$ -labeled side chain.<sup>22</sup> Therefore, at therapeutic dosage levels for intact whole cells,

the isotridecanyl side chain of  $[^2\text{H}]\text{pb-A}_3$  does not mediate the binding of drug to the membrane or the formation of a drug-aggregated membrane pore structure. Instead, we find  $[^2\text{H}]\text{pb-A}_3$  localized within the cell wall. The dipolar contact between the deuterium labels of  $[^2\text{H}]\text{pb-A}_3$  and the carbonyl carbon labels of  $[1\text{-}^{13}\text{C}]\text{glycine}$  in the peptidoglycan cross bridge (Figure 3, right) shows unambiguously that the isotridecanyl side chain is involved in cell-wall binding.

The addition of  $[^2\text{H}]\text{pb-A}_3$  (11.8  $\mu\text{g/mL}$ ) to whole cells of *S. aureus* during the midexponential growth ( $\text{OD}_{660}$  at 0.5) showed no inhibition of the transpeptidation step of peptidoglycan biosynthesis (Figure 4 and Figure S3 of the Supporting Information). Although transpeptidase inhibition may occur at higher drug concentrations, the accumulation of a cytoplasmic peptidoglycan precursor (Park's nucleotide) and inhibition of purine biosynthesis (Figures 4 and 5) are consistent with  $[^2\text{H}]\text{pb-A}_3$  acting primarily as a transglycosylase inhibitor in *S. aureus*.

We also found that  $[^2\text{H}]\text{pb-A}_3$  inhibited the incorporation of D- $[1\text{-}^{13}\text{C}]\text{alanine}$  into cell-wall teichoic acids (Figure 7). Similar inhibition of peptidoglycan and teichoic acid biosynthesis has been observed for *S. aureus* cells treated with vancomycin and oritavancin.<sup>19</sup> Such dual inhibition may be due to drug targeting of lipid II (or the membrane-associated nascent peptidoglycan) and the resulting unavailability of lipid transporter bactoprenol phosphate.<sup>23</sup> Because  $[^2\text{H}]\text{pb-A}_3$  is fully active only in the presence of the intact cell wall, a conventional inhibition assay based on isolated, purified enzymes and substrates could miss the dual inhibition.

The molecular role of the isotridecanyl side chain in  $[^2\text{H}]\text{pb-A}_3$  for transglycosylase inhibition remains unknown. However, the drug side chain is essential for antimicrobial activity. The MICs of  $\text{pb-A}_3$  and *deslipo-pb-A}\_3* ( $\text{pb-A}_3$  without the isotridecanyl side chain) show *deslipo-pb-A}\_3* has no antimicrobial activity (Table S1 of the Supporting Information). The isotridecanyl side chain may simply act as a steric blocker, preventing substrates from reaching the transglycosylase active site.<sup>24</sup> A similar role has been suggested<sup>17</sup> for the hydrophobic side chain of oritavancin, which inserts in cell-wall-free bilayers but not in the bilayers of whole cells.<sup>22</sup>

## ■ ASSOCIATED CONTENT

### ■ Supporting Information

A description of the synthesis of  $[^2\text{H}]\text{pb-A}_3$ , minimal inhibitory concentrations (micrograms per milliliter) of  $\text{pb-A}_3$ , *deslipo-pb-A}\_3*, and  $[^2\text{H}]\text{pb-A}_3$  (Table S1), retrosynthetic analysis for  $[^2\text{H}]\text{pb-A}_3$  (Figure S1), preparation of isotopically labeled depsipeptide fragment 5 (Figure S2), and 20.3 MHz  $^{15}\text{N}\{^{13}\text{C}\}$  REDOR spectra after dipolar evolution for 1.6 ms of whole cells of *S. aureus* grown in a defined medium containing D- $[1\text{-}^{13}\text{C}]\text{alanine}$  and  $[^{15}\text{N}]\text{glycine}$  in the absence (left) and presence of  $[^2\text{H}]\text{pb-A}_3$  (right) (Figure S3). This material is available free of charge via the Internet at <http://pubs.acs.org>.

## ■ AUTHOR INFORMATION

### Corresponding Author

\*Phone: (314) 935-6844. Fax: (314) 935-4481. E-mail: [jschaefer@wustl.edu](mailto:jschaefer@wustl.edu).

### Funding

This paper is based on work supported by National Institutes of Health Grants AI059327 (M.V.) and EB002058 (J.S.).

## Notes

The authors declare no competing financial interest.

## ■ ABBREVIATIONS

$^{13}\text{C}\{^2\text{H}\}$  or  $\text{C}\{\text{D}\}$ , carbon channel observation with deuterium dephasing;  $^{13}\text{C}\{^{15}\text{N}\}$  or  $\text{C}\{\text{N}\}$ , carbon channel observation with nitrogen dephasing;  $^{15}\text{N}\{^{13}\text{C}\}$  or  $\text{N}\{\text{C}\}$ , nitrogen channel observation with carbon dephasing;  $^{31}\text{P}\{^2\text{H}\}$  or  $\text{P}\{\text{D}\}$ , phosphorus channel observation with deuterium dephasing; REDOR, rotational-echo double resonance.

## ■ REFERENCES

- (1) Shoji, J., Hinoo, H., Katayama, T., Matsumoto, K., Tanimoto, T., Hattori, T., Higashiyama, I., Miwa, H., Motokawa, K., and Yoshida, T. (1992) Isolation and characterization of new peptide antibiotics, plusbacins A1-A4 and B1-B4. *J. Antibiot.* 45, 817–823.
- (2) Maki, H., Miura, K., and Yamano, Y. (2001) Katanosin B and plusbacin A<sub>3</sub>, inhibitors of peptidoglycan synthesis in methicillin-resistant *Staphylococcus aureus*. *Antimicrob. Agents Chemother.* 45, 1823–1827.
- (3) Wohrlab, A., Lamer, R., and VanNieuwenhze, M. S. (2007) Total synthesis of plusbacin A<sub>3</sub>: A depsipeptide antibiotic active against vancomycin-resistant bacteria. *J. Am. Chem. Soc.* 129, 4175–4177.
- (4) Straus, S. K., and Hancock, R. E. (2006) Mode of action of the new antibiotic for Gram-positive pathogens daptomycin: Comparison with cationic antimicrobial peptides and lipopeptides. *Biochim. Biophys. Acta* 1758, 1215–1223.
- (5) Gullion, T., and Schaefer, J. (1989) Rotational-echo double-resonance NMR. *J. Magn. Reson.* 81, 196–200.
- (6) Tong, G., Pan, Y., Dong, H., Pryor, R., Wilson, G. E., and Schaefer, J. (1997) Structure and dynamics of pentaglycyl bridges in the cell walls of *Staphylococcus aureus* by  $^{13}\text{C}\text{-}^{15}\text{N}$  REDOR NMR. *Biochemistry* 36, 9859–9866.
- (7) Kim, S. J., Cegelski, L., Studelska, D. R., O'Connor, R. D., Mehta, A. K., and Schaefer, J. (2002) Rotational-echo double resonance characterization of vancomycin binding sites in *Staphylococcus aureus*. *Biochemistry* 41, 6967–6977.
- (8) Bennett, A. E., Reienstra, C. M., Auger, M., Lakshmi, K. V., and Griffin, R. G. (1995) Heteronuclear decoupling in rotating solids. *J. Chem. Phys.* 103, 6951–6958.
- (9) Stueber, D., Mehta, A. K., Chen, Z., Wooley, K. L., and Schaefer, J. (2006) Local order in polycarbonate glasses by  $^{13}\text{C}\{^{19}\text{F}\}$  Rotational-Echo Double-Resonance NMR. *J. Polym. Sci., Part B: Polym. Phys.* 44, 2760–2775.
- (10) Gullion, T., Baker, D. B., and Conradi, M. S. (1990) New, compensated Carr-Purcell sequences. *J. Magn. Reson.* 89, 479–484.
- (11) Wedeghiorgis, T. K., and Schaefer, J. (2003) Compensating for pulse imperfections in REDOR. *J. Magn. Reson.* 165, 230–236.
- (12) Mueller, K. T., Jarvie, T. P., Aurentz, D. J., and Roberts, B. W. (1995) The REDOR transform: Direct calculation of internuclear couplings from dipolar-dephasing NMR data. *Chem. Phys. Lett.* 242, 535–542.
- (13) Goetz, J. M., and Schaefer, J. (1997) REDOR dephasing by multiple spins in the presence of molecular motion. *J. Magn. Reson.* 127, 147–154.
- (14) Kim, S. J., Cegelski, L., Preobrazhenskaya, M., and Schaefer, J. (2006) Structures of *Staphylococcus aureus* cell-wall complexes with vancomycin, eremomycin, and chloroeremomycin derivatives by  $^{13}\text{C}\text{-}\{^{19}\text{F}\}$  and  $^{15}\text{N}\{^{19}\text{F}\}$  rotational-echo double resonance. *Biochemistry* 45, 5235–5250.
- (15) Paik, Y., Yang, C., Metaferia, B., Tang, S., Bane, S., Ravindra, R., Shanker, N., Alcaraz, A. A., Johnson, S. A., Schaefer, J., O'Connor, R. D., Cegelski, L., Snyder, J. P., and Kingston, D. G. (2007) Rotational-echo double-resonance NMR distance measurements for the tubulin-bound Paclitaxel conformation. *J. Am. Chem. Soc.* 129, 361–370.
- (16) Lewis, B. A., and Engelman, D. M. (1983) Lipid bilayer thickness varies linearly with acyl chain length in fluid phosphatidylcholine vesicles. *J. Mol. Biol.* 166, 211–217.

- (17) Kim, S. J., Cegelski, L., Stueber, D., Singh, M., Dietrich, E., Tanaka, K. S., Parr, T. R., Far, A. R., and Schaefer, J. (2008) Oritavancin exhibits dual mode of action to inhibit cell-wall biosynthesis in *Staphylococcus aureus*. *J. Mol. Biol.* 377, 281–293.
- (18) Cegelski, L., Kim, S. J., Hing, A. W., Studelska, D. R., O'Connor, R. D., Mehta, A. K., and Schaefer, J. (2002) Rotational-echo double resonance characterization of the effects of vancomycin on cell wall synthesis in *Staphylococcus aureus*. *Biochemistry* 41, 13053–13058.
- (19) Cegelski, L., Steuber, D., Mehta, A. K., Kulp, D. W., Axelsen, P. H., and Schaefer, J. (2006) Conformational and quantitative characterization of oritavancin-peptidoglycan complexes in whole cells of *Staphylococcus aureus* by in vivo <sup>13</sup>C and <sup>15</sup>N labeling. *J. Mol. Biol.* 357, 1253–1262.
- (20) Baltz, R. H., Miao, V., and Wrigley, S. K. (2005) Natural products to drugs: Daptomycin and related lipopeptide antibiotics. *Nat. Prod. Rep.* 22, 717–741.
- (21) Silverman, J. A., Perlmutter, N. G., and Shapiro, H. M. (2003) Correlation of Daptomycin Bacterial Activity and Membrane Depolarization in *Staphylococcus aureus*. *Antimicrob. Agents Chemother.* 47, 2538–2544.
- (22) Kim, S. J., Singh, M., and Schaefer, J. (2009) Oritavancin binds to isolated protoplast membranes but not intact protoplasts of *Staphylococcus aureus*. *J. Mol. Biol.* 391, 414–425.
- (23) Schneider, T., and Sahl, H. G. (2010) Lipid II and other bactoprenol-bound cell wall precursors as drug targets. *Curr. Opin. Invest. Drugs* 11, 157–164.
- (24) Kim, S. J., Matsuoka, S., Patti, G. J., and Schaefer, J. (2008) Vancomycin derivative with damaged D-Ala-D-Ala binding cleft binds to cross-linked peptidoglycan in the cell wall of *Staphylococcus aureus*. *Biochemistry* 47, 3822–3831.